DALTON
FULL PAPER

Nitrile functionalised pendant-arm derivatives of aza- and mixed donor macrocyclic ligands as new building blocks for inorganic crystal engineering

Lorenzo Tei,[a,b] Alexander J. Blake,[a] Paul A. Cooke,[a] Claudia Caltagirone,[b] Francesco Demartin,[c] Vito Lippolis,*[b] Francesca Morale,[a] Claire Wilson[a] and Martin Schröder *[a]

[a] *School of Chemistry, The University of Nottingham, University Park, Nottingham, UK NG7 2RD*
[b] *Dipartimento di Chimica Inorganica ed Analitica, Università degli studi di Cagliari, SS 554 Bivio per Sestu, 09042 Monserrato (Ca), Italy*
[c] *Dipartimento di Chimica Strutturale e Stereochimica Inorganica, Università di Milano, Via G. Venezian 21, 20133 Milano, Italy*

Received 16th November 2001, Accepted 24th January 2002
First published as an Advance Article on the web 26th March 2002

A range of nitrile-functionalised pendant arm derivatives of [9]aneN$_3$, [9]aneN$_2$S, [9]aneNS$_2$, [12]aneNS$_2$O and [15]aneO$_2$N$_3$ have been prepared: L^1 = 1,4,7-tris(cyanomethyl)-1,4,7-triazacyclononane, L^2 = 1,4,7-tris-(2-cyanoethyl)-1,4,7-triazacyclononane, L^3 = 1,2-bis[4,7-bis(2-cyanoethyl)-1,4,7-triazacyclonon-1yl]ethane, L^4 = 4,7-bis(2-cyanoethyl)-1-thia-4,7-diazacyclononane, L^5 = 7-(2-cyanoethyl)-7-aza-1,4-dithiacyclononane, L^6 = 1-(2-cyanoethyl)-1-aza-4,10-dithia-7-oxacyclododecane, L^7 = 1,4,7-tris(cyanomethyl)-1,4,7-triaza-10,13-dioxacyclopentadecane, L^8 = 1,4,7-tris(cyanoethyl)-1,4,7-triaza-10,13-dioxacyclopentadecane. Reaction of these ligands with Ag^I salts affords a range of complex products, the structures of which vary according to the type, number and length of the pendant arms. The synthesis and structures of {[Ag(L^1)]PF$_6$}$_\infty$, {[Ag$_2$(L^2)$_2$][BF$_4$]$_2$}$_\infty$, {[Ag$_2$(L^3)][PF$_6$]$_2$}$_\infty$, [Ag$_2$(L^4)$_2$][BF$_4$]$_2$, {[Ag(L^5)]BF$_4$}$_\infty$, [Ag$_2$(L^6)$_2$][BF$_4$]$_2$, {[Ag(L^7)]BF$_4$}$_\infty$ and [Ag(L^8)]PF$_2$O$_2$ are reported.

Introduction

The field of crystal engineering and the design of 2D and 3D inorganic co-ordination polymers is receiving growing attention.[1–6] Rigid rod-like bidentate ligands such as 4,4′-bipyridyl and its analogues are usually used to connect late transition metal centres and the resulting co-ordination polymers have been shown to form a wide range of interesting network topologies ranging from chains to ladders, grids and adamantoid arrays.[2,6] The effects on the structure of co-ordination networks exerted by inter-ligand π–π interactions, the nature of the anion, solvent and the reaction molar ratios have to be carefully considered.[2,7] The design and synthesis of new multidentate ligands to be used as building blocks for the construction of desired solid-state architectures remain therefore major targets.

Functionalised pendant-arm derivatives of aza-crown ethers have been used extensively as ligands for the preparation of complexes of high kinetic inertness and thermodynamic stability, such complexes often exhibiting specific co-ordination and redox properties.[8–13] Pendant groups are often attached to the macrocyclic framework in order to promote endocyclic complexation. We have initiated a study of functionalised pendant arm macrocyclic ligands in order to assemble and construct, for the first time, multidimensional exocyclic solid-state architectures.[14] We report herein the co-ordination properties of the ligands L^1–L^8 (Scheme 1) with Ag^I. We argued that nitrile-containing pendant arms would prevent these polydentate ligands forming sandwich complexes and would promote the formation of polymeric framework compounds.

Results and discussion

Reaction of one molar equivalent of AgPF$_6$ with L^1 gives the polymeric complex {[Ag(L^1)]PF$_6$}$_\infty$,[14] in which the Ag^I ion is bound to six N-donors in a distorted octahedral geometry. One face is taken up by the three N-donors of the triaza ring, [Ag–N 2.523(4)–2.547(4) Å (Fig. 1, Table 1)], with the remaining three

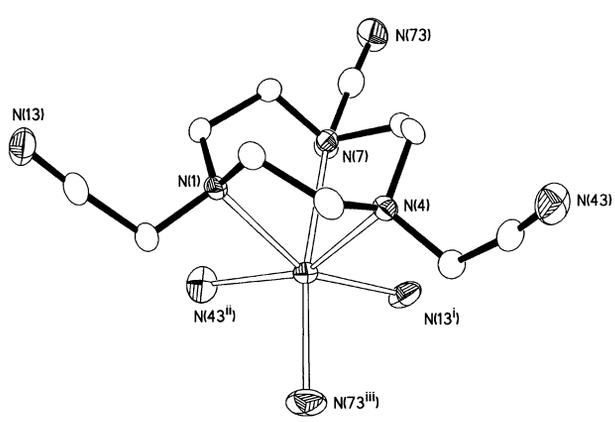

Fig. 1 View of the co-ordination sphere in the cation of [Ag(L^1)]PF$_6$ with the numbering scheme adopted. The nitrogen atoms N(13^i), N(43^{ii}) and N(73^{iii}) belong to three different symmetry-related molecules of L^1 [i = ½ + x, ³⁄₂ − y, −½ + z; ii = −½ + x, ³⁄₂ − y, −½ + z; iii = ½ − x, ½ + y, ½ − z]. Hydrogen atoms and the PF$_6^-$ counter ion are omitted for clarity and displacement ellipsoids are drawn at 50% probability.

positions occupied by the N-donors of nitrile groups belonging to three different [Ag(L^1)]$^+$ ions, [Ag–N 2.311(4)–2.486(4) Å]. A three-dimensional inorganic network is, therefore, formed in which each molecule of L^1 is linked to four separate Ag^I centres with each Ag^I ion representing a six-connected junction *via* NCH$_2$CN linkers in an overall three dimensional single network (Fig. 2). Interestingly, the structure of this polymeric cationic network does not depend upon whether BF$_4^-$ or PF$_6^-$ is the

 DOI: 10.1039/b110134j

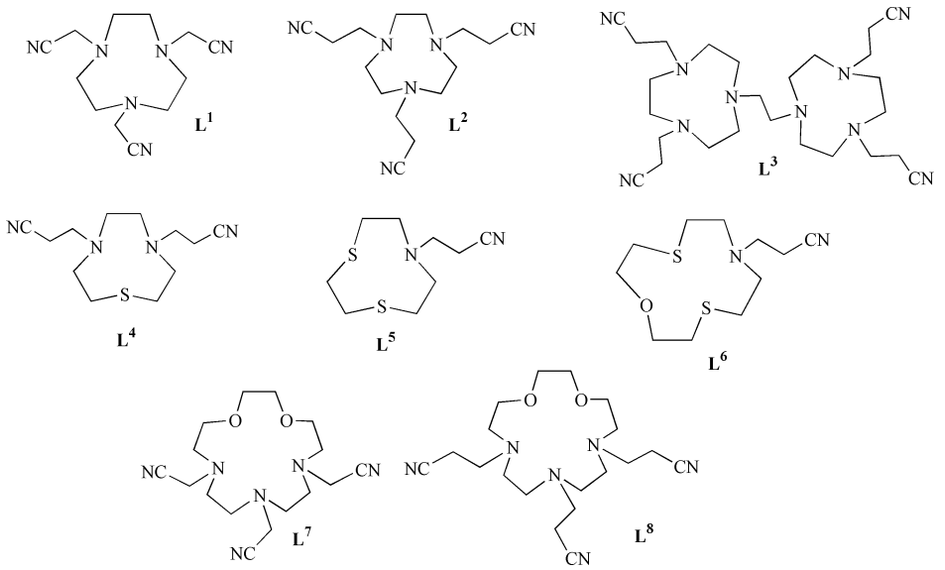

Scheme 1

Table 1 Selected bond distances (Å) and angles (°) for $\{[Ag(L^1)]PF_6\}_\infty$

Ag(1)–N(1)	2.547(4)	Ag(1)–N(4)	2.523(4)
Ag(1)–N(7)	2.532(4)	Ag(1)–N(13^{iii})	2.486(4)
Ag(1)–N(43^{ii})	2.415(4)	Ag(1)–N(73^{i})	2.311(4)
N(1)–Ag(1)–N(4)	70.92(12)	N(1)–Ag(1)–N(7)	71.34(11)
N(1)–Ag(1)–N(13^{iii})	15.53(13)	N(1)–Ag(1)–N(43^{ii})	83.16(13)
N(1)–Ag(1)–N(73^{i})	115.67(14)	N(4)–Ag(1)–N(7)	71.38(12)
N(4)–Ag(1)–N(13^{iii})	97.34(14)	N(4)–Ag(1)–N(43^{ii})	153.20(13)
N(4)–Ag(1)–N(73^{i})	104.1(2)	N(7)–Ag(1)–N(13^{iii})	83.58(13)
N(7)–Ag(1)–N(43^{ii})	94.3(2)	N(7)–Ag(1)–N(73^{i})	170.5(2)
N(13^{iii})–Ag(1)–N(43^{ii})	103.6(2)	N(13^{iii})–Ag(1)–N(73^{i})	88.8(2)
N(73^{i})–Ag(1)–N(43^{ii})	93.0(2)		

Symmetry operations: i = ½ + x, ³⁄₂ − y, −½ + z; ii = −½ + x, ³⁄₂ − y, −½ + z; iii = ½ − x, ½ + y, ½ − z.

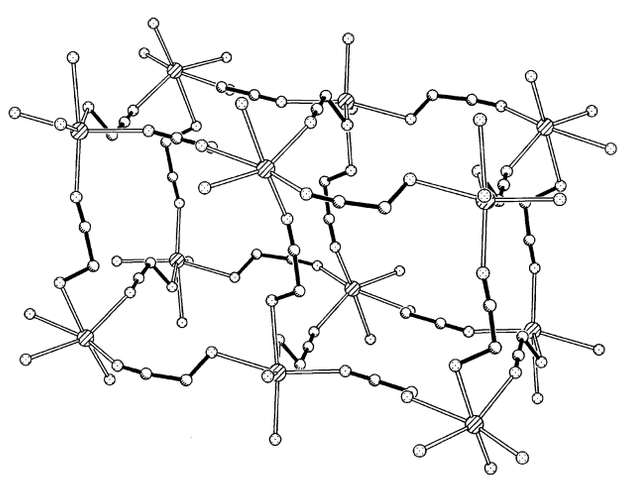

Fig. 2 Partial view of the $\{[Ag(L^1)]^+\}_\infty$ three-dimensional polymer: the methylene units belonging to the [9]aneN$_3$ frameworks and counter anions are omitted for clarity to better show the six-connected single network at Ag^{I} centres.

counter anion since the channels within the polymer can accommodate both anions. Six-connected single networks at Ag^{I} consisting of a cationic frame linked by molecular rods are very rare, the only reported example being the complex $[Ag(pyz)_3]SbF_6$ (pyz = pyrazine) which is topologically related to the structure of ReO_3 or Prussian blue.[15]

In the light of this result, the ligand L^2, which differs from L^1 in having one more methylene group in each pendant arm, was treated with $AgBF_4$ in a 1 : 1 molar ratio in MeCN.[14] Although analytical and mass spectrometric data for the product are consistent with the stoichiometry $[Ag(L^2)]BF_4$, a single crystal structure determination was undertaken to ascertain the ligation and nuclearity of the product. The determination confirms the product to be a one-dimensional zigzag polymer, $\{[Ag_2(L^2)_2][BF_4]_2\}_\infty$ in which the repeating unit is the binuclear complex cation $[Ag_2(L^2)_2]^{2+}$ lying across a crystallographic inversion centre (Fig. 3). Each Ag^{I} centre is bound to four

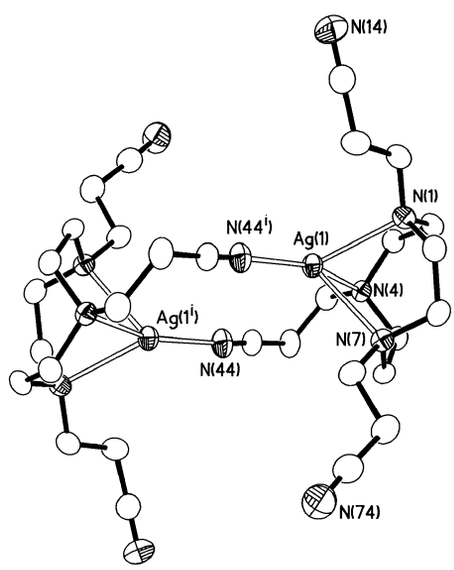

Fig. 3 View of the binuclear cation in $[Ag_2(L^2)_2][BF_4]_2$ with numbering scheme adopted. Hydrogen atoms and counter ions are omitted for clarity and displacement ellipsoids are drawn at 50% probability [i = 1 − x, 1 − y, −z].

N-donors in a distorted tetrahedral geometry with N–Ag–N angles ranging from 73.80(2) [N(1)–Ag(1)–N(7)] to 159.1(2)° [N(4)–Ag(1)–N(44^{i})] and Ag–N bond distances from 2.192(6) [Ag(1)–N(44^{i})] to 2.504(5) Å [Ag(1)–N(7)] (Table 2). Three N-donors are provided by the [9]aneN$_3$ framework of L^2 and the fourth, which completes the co-ordination sphere around the metal centre, comes from the nitrile group of a pendant arm from a symmetry-related $[Ag(L^2)]^+$ unit (Fig. 3). One of the two remaining pendant arms of L^2 interacts with a Ag^{I} centre of an inversion-related $[Ag_2(L^2)_2]^{2+}$ binuclear fragment [Ag(1)–N(14^{ii}) 2.779(7) Å] to give an infinite zigzag polymer along the a axis (Fig. 4). Thus, by simply altering the pendant arm length from CH_2CN in L^1 to CH_2CH_2CN in L^2, a different network motif for the resultant co-ordination polymer with Ag^{I} is formed.

Table 2 Selected bond distances (Å) and angles (°) for $\{[Ag_2(L^2)_2][BF_4]_2\}_\infty$

Ag(1)–N(1)	2.450(5)	Ag(1)–N(4)	2.412(5)
Ag(1)–N(7)	2.504(5)	Ag(1)–N(44^{i})	2.192(6)
Ag(1)–N(14^{ii})	2.779(7)		
N(1)–Ag(1)–N(4)	76.33(2)	N(1)–Ag(1)–N(7)	73.80(2)
N(4)–Ag(1)–N(7)	74.01(2)	N(1)–Ag(1)–N(44^{i})	124.4(2)
N(4)–Ag(1)–N(44^{i})	159.1(2)	N(7)–Ag(1)–N(44^{i})	111.8(2)
N(1)–Ag(1)–N(14^{ii})	93.1(2)	N(4)–Ag(1)–N(14^{ii})	87.8(2)
N(7)–Ag(1)–N(14^{ii})	159.5(2)	N(44^{i})–Ag(1)–N(14^{ii})	88.6(2)

Symmetry operations: i = 1 − *x*, 1 − *y*, −*z*; ii = 2 − *x*, 1 − *y*, −*z*.

Table 3 Selected bond distances (Å) and angles (°) for $\{[Ag_2(L^3)][PF_6]_2\}_\infty$

Ag–N(1)	2.476(3)	Ag–N(4)	2.464(4)
Ag–N(7)	2.483(3)	Ag–N(44^{ii})	2.262(4)
Ag–N(74^{iii})	2.501(4)		
N(1)–Ag–N(4)	75.10(12)	N(1)–Ag–N(7)	73.13(11)
N(1)–Ag–N(44^{ii})	105.2(2)	N(1)–Ag–N(74^{iii})	170.56(13)
N(4)–Ag–N(7)	74.52(12)	N(4)–Ag–N(44^{ii})	153.55(14)
N(4)–Ag–N(74^{iii})	103.2(2)	N(7)–Ag–N(44^{ii})	131.46(13)
N(7)–Ag–N(74^{ii})	97.44(13)	N(44^{ii})–Ag–N(74^{iii})	80.6(2)

Symmetry operations: i = 1 − *x*, 1 − *y*, 1 − *z*; ii = −*x*, 1 − *y*, 1 − *z*; iii = −*x*, −*y*, 1 − *z*; iv = 1 + *x*, *y*, *z*; v = 1 + *x*, 1 + *y*, *z*.

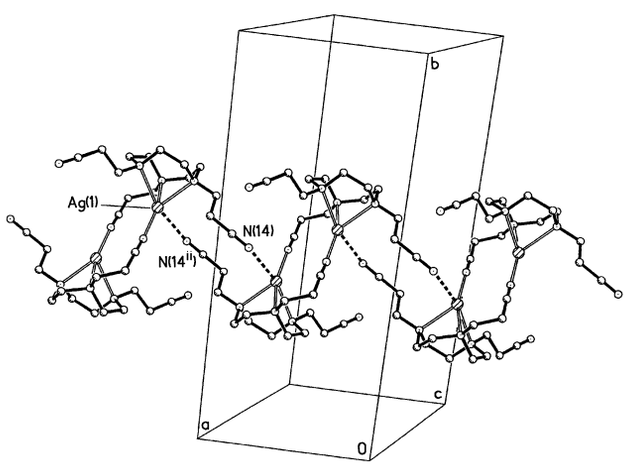

Fig. 4 Packing diagram for $\{[Ag_2(L^2)_2]^{2+}\}_\infty$ polymeric chains. Counter anions are omitted for clarity [ii = 2 − *x*, 1 − *y*, −*z*].

We argued that nitrile pendant-arm derivatives of bis([9]aneN$_3$) ligands would represent a further step in the design of new flexible ligands suitable for the synthesis of inorganic polymers. We therefore treated L^3 with two molar equivalents of $AgPF_6$ in MeCN at room temperature to afford a product of formulation $[Ag_2(L^3)][PF_6]_2$. Single crystals of diffraction quality were grown by diffusing Et_2O into a solution of the complex in MeCN. The X-ray crystal structure determination confirms each [9]aneN$_3$ moiety in the ligand hosts one Ag^I centre (Fig. 5). Each Ag^I ion in the complex cation $[Ag_2(L^3)]^{2+}$ is bound to five N-donors in a highly distorted trigonal bipyramidal co-ordination geometry, with one axial position and two equatorial positions taken up by the three N-donors of the triaza ring moiety [Ag–N 2.464(4)–2.483(3) Å]. The remaining axial [Ag–N(74^{iii}) 2.501(4) Å] and equatorial [Ag–N(44^{ii}) 2.262(4) Å] sites are occupied by the N-donors of nitrile groups from two different $[Ag_2(L^3)]^{2+}$ centres (Table 3). The two pentadentate compartments of L^3 are arranged in an *anti*-configuration similar to that found for most other binuclear complexes of bis([9]aneN$_3$) ligands with functionalised different pendant arms.[12,13,16] Thus, a two-dimensional inorganic network is observed for the complex in which each $[Ag_2(L^3)]^{2+}$ unit is linked through two metal centres to four symmetry-related units (Fig. 6) with pairs of linked $[Ag_2(L^3)]^{2+}$ units sharing two nitrile pendant arms. In this way each penta-co-ordinate Ag^I ion is connected to two other Ag^I centres through two NCH_2CH_2CN linkers and to a third metal centre *via* an NCH_2CH_2N linker (Fig. 6). A better insight into the nature of the resulting network can be obtained by omitting the carbon atoms of the [9]aneN$_3$ moieties. Ribbons of fused 12-membered rings connected at Ag^I spiro-centres can then be envisaged within a two-dimensional architecture (Fig. 7). Each ring comprises two metal centres and the two NCH_2CH_2CN linkers connecting them, with the mean planes containing consecutive 12-membered rings almost perpendicular to each other. The resulting ribbons running along the [010] direction are stacked along [100], and are connected at the metal centres *via* NCH_2CH_2N linkers. In terms of connectivity, the two-dimensional network is perhaps best viewed as a distorted "brick-wall" structure constructed using two different type of linkers, with the single bridge running in the [100] direction and the double bridge in the [010] direction (Scheme 2).

As a continuation of these studies with ligands showing different degrees of functionality, we have also explored the co-ordination chemistry of the analogous derivatives of [9]aneN$_2$S (L^4) and [9]aneNS$_2$ (L^5) (Scheme 1) towards Ag^I.

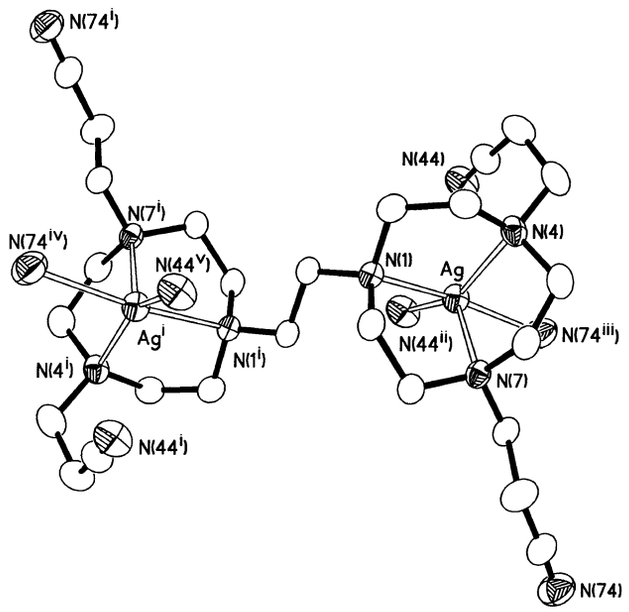

Fig. 5 View of the co-ordination sphere around the Ag^I ions in the cation of $[Ag_2(L^3)][PF_6]_2$ with the numbering scheme adopted. The nitrogen atoms N(44^{ii}), N(74^{iii}), N(74^{iv}) and N(44^{v}) belong to four different symmetry-related molecules of L^3 [i = 1 − *x*, 1 − *y*, 1 − *z*; ii = −*x*, 1 − *y*, 1 − *z*; iii = −*x*, −*y*, 1 − *z*; iv = 1 + *x*, *y*, *z*; v = 1 + *x*, 1 + *y*, *z*]. Hydrogen atoms and counter ions are omitted for clarity and displacement ellipsoids are drawn at 50% probability.

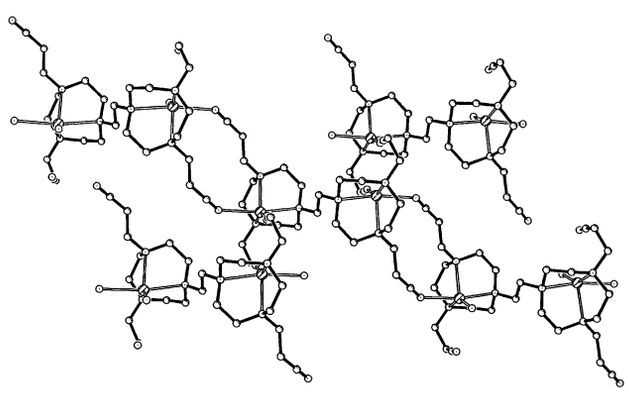

Fig. 6 Packing diagram showing part of the $\{[Ag_2(L^3)]^{2+}\}_\infty$ two-dimensional polymer.

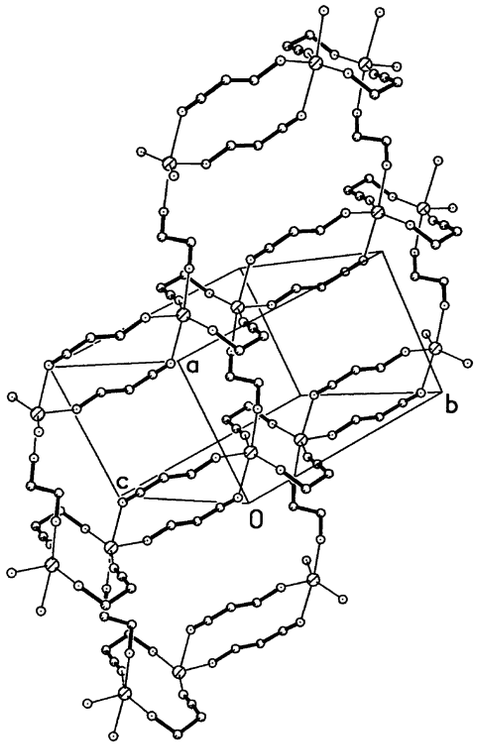

Fig. 7 Packing diagram showing part of the $\{[Ag_2(L^3)]^{2+}\}_\infty$ two-dimensional polymer with the carbon atoms of the [9]aneN$_3$ moieties being omitted for clarity.

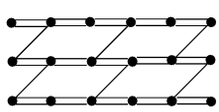

Scheme 2

Reaction of L^4 with $AgBF_4$ in a 1 : 1 molar ratio in MeCN at room temperature gives colourless blocky crystals after partial removal of the solvent and subsequent diffusion of Et_2O vapour into the remaining solution. Microanalytical data support the formulation $[Ag(L^4)]BF_4$ for the isolated compound; however, FAB mass spectra show molecular ion peaks corresponding to the binuclear species $[Ag_2(L^4)_2][BF_4]_2$. A single crystal X-ray structure determination confirms the product to be a discrete binuclear Ag^I complex (Fig. 8) in which each Ag^I ion in the binuclear cation $[Ag_2(L^4)_2]^{2+}$ is co-ordinated to three N-donors and one S-donor in a very distorted tetrahedral geometry with bond angles ranging from 73.09(7) [N(4)–Ag(1)–N(7)] to 159.26(7)° [S(1)–Ag(1)–N(44^i)]. Ag–N bond distances lie between 2.166(2) [Ag(1)–N(44^i)] and 2.539(2) Å [Ag(1)–N(4)] with a Ag(1)–S(1) bond length of 2.4834(8) Å (Table 4). Because of the large S(1)–Ag(1)–N(44^i) angle, a saw-horse description can also be adopted for the co-ordination geometry around the metal centre. Two out of three N-donors are provided by the [9]aneN$_2$S macrocyclic framework, while the third N-donor, which together with a S-donor from the ring system completes the co-ordination sphere around the metal centre, comes from the nitrile group of a pendant arm of a symmetry-related $[Ag(L^4)]^+$ unit (Fig. 8). The structure, therefore, confirms that two inversion-related $[Ag(L^4)]^+$ units are held together within the binuclear complex by Ag–N bonds involving one nitrile functionalised pendant arm from each ligand, with the remaining two pendant arms being left uncoordinated. As for $[Ag_2(L^2)_2]^{2+}$ (Fig. 3) and $\{[Ag_2(L^3)]^{2+}\}_\infty$ (Figs. 6 and 7), a 12-membered metallocycle incorporating two NCH_2CH_2CN linkers and the two Ag^I centres is observed for $[Ag_2(L^4)_2][BF_4]_2$. Indeed, the structure of $[Ag_2(L^4)_2]^{2+}$ is very similar to that observed for $[Ag_2(L^2)_2]^{2+}$ (Fig. 3), the main difference being the presence of additional interactions between binuclear $[Ag_2(L^2)_2]^{2+}$ fragments *via* nitrile groups to give a polymeric architecture (Fig. 4). This can be attributed to the presence of only two nitrile arms in L^4 rather than three as in L^2. Indeed, the third pendant arm in L^2, which has been substituted by an S-donor in L^4, can be considered formally as being responsible for the observed polymeric structure in $\{[Ag_2(L^2)_2]^{2+}\}_\infty$ (Fig. 4).

Table 4 Selected bond distances (Å) and angles (°) for $[Ag_2(L^4)_2][BF_4]_2$

Ag(1)–N(4)	2.539(2)	Ag(1)–N(7)	2.470(2)
Ag(1)–S(1)	2.4834(8)	Ag(1)–N(44^i)	2.166(2)
N(4)–Ag(1)–N(7)	73.09(7)	N(4)–Ag(1)–S(1)	79.90(5)
N(7)–Ag(1)–S(1)	82.57(5)	N(4)–Ag(1)–N(44^i)	106.21(8)
N(7)–Ag(1)–N(44^i)	118.13(8)	S(1)–Ag(1)–N(44^i)	159.26(7)

Symmetry operations: i = $-x, -y, -z$.

In order to understand and appreciate better the effect of the number of nitrile functionalised pendant arms on the co-ordination chemistry of functionalised mixed thia–aza nine-membered rings towards Ag^I, we also treated L^5 with $AgBF_4$. L^5 has only one nitrile functionalised pendant arm, but the formation of binuclear complexes analogous to $\{[Ag_2(L^2)_2]^{2+}\}_\infty$ and $[Ag_2(L^4)_2]^{2+}$ should still be possible. Although analytical and mass spectrometric data for the isolated product were consistent with the stoichiometry $[Ag(L^5)]BF_4$, a single crystal structure determination confirmed the absence of binuclear aggregates and shows the formation of a one-dimensional sinusoidal polymer, $\{[Ag(L^5)]BF_4\}_\infty$, in which the repeating unit is the mononuclear complex cation $[Ag(L^5)]^+$ (Fig. 9). Each Ag^I ion in the polymer is bound by a [2S + N] donor set from the

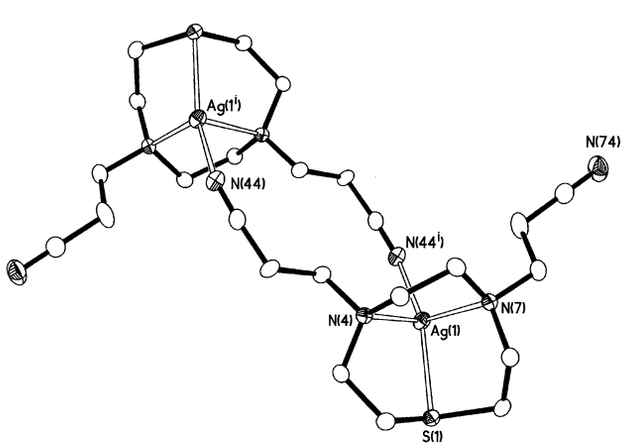

Fig. 8 View of the binuclear cation in $[Ag_2(L^4)_2][BF_4]_2$ with the numbering scheme adopted. Hydrogen atoms and counter ions are omitted for clarity and displacement ellipsoids are drawn at 50% probability [i = $-x, -y, -z$].

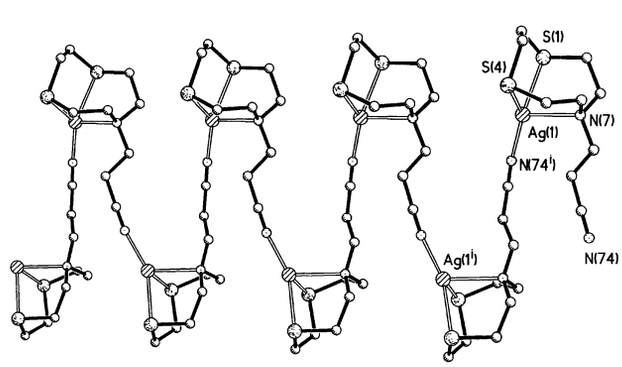

Fig. 9 Packing diagram for the $\{[Ag(L^5)]BF_4\}_\infty$ polymeric chain running along the *b* axis with the numbering scheme adopted. Hydrogen atoms and counter anions are omitted for clarity [i = ½ − *x*, ½ + *y*, ⅔ − *z*].

Table 5 Selected bond distances (Å) and angles (°) for $\{[Ag(L^5)]BF_4\}_\infty$

Ag(1)–N(7)	2.459(4)	Ag(1)–S(1)	2.5551(13)
Ag(1)–S(4)	2.5423(13)	Ag(1)–N(74^i)	2.153(4)
N(7)–Ag(1)–S(1)	81.27(9)	N(7)–Ag(1)–S(4)	81.36(9)
S(1)–Ag(1)–S(4)	87.19(4)	N(7)–Ag(1)–N(74^i)	111.2(2)
S(1)–Ag(1)–N(74^i)	136.09(12)	S(4)–Ag(1)–N(74^i)	135.18(12)

Symmetry operations: i = ½ − x, ½ + y, $\frac{3}{2}$ − z.

Table 6 Selected bond distances (Å) and angles (°) for $[Ag_2(L^6)_2][BF_4]_2$

Ag(1)–N(1)	2.508(4)	Ag(1)–S(4)	2.529(2)
Ag(1)–S(10)	2.600(2)	Ag(1)–O(7)	2.788(6)
Ag(1)–N($4A^i$)	2.266(4)		
N(1)–Ag(1)–N($4A^i$)	107.66(14)	N(1)–Ag(1)–S(4)	81.11(10)
N(1)–Ag(1)–S(10)	80.12(10)	N(1)–Ag(1)–O(7)	112.8(2)
S(4)–Ag(1)–N($4A^i$)	121.19(12)	S(4)–Ag(1)–S(10)	129.29(5)
S(4)–Ag(1)–O(7)	75.19(14)	S(10)–Ag(1)–N($4A^i$)	109.34(12)
S(10)–Ag(1)–O(7)	69.74(14)	O(7)–Ag(1)–N($4A^i$)	138.4(2)

Symmetry operations: i = 2 − x, 2 − y, −z.

[9]aneNS$_2$ macrocyclic framework and by the nitrile group of a symmetry-related $[Ag(L^5)]^+$ unit. Thus, sinusoidal polymeric chains featuring tetrahedrally co-ordinated Ag^I ions connected by NCH$_2$CH$_2$CN linkers run along the *b* axis. Interestingly, for all three compounds obtained from the reaction of $AgBF_4$ with L^2, L^4 and L^5, the shortest Ag–N bond distances are those involving bridging nitrile groups. Furthermore, the tetrahedral co-ordination geometry at the metal centre in $\{[Ag(L^5)]^+\}_\infty$ is less distorted (Table 5) than that observed for the Ag^I ions in the complexes $\{[Ag_2(L^2)_2]^{2+}\}_\infty$ and $[Ag_2(L^4)_2]^{2+}$ (Tables 2 and 4); this can be rationalised by the additional steric and angular constraints imposed by the formation of the 12-membered metallocyclic ring in both $\{[Ag_2(L^2)_2]^{2+}\}_\infty$ and $[Ag_2(L^4)_2]^{2+}$. Thus, reaction of Ag^I salts with nitrile-functionalised 9-membered ring macrocycles affords a range of complexes the topologies of which are closely controlled by the nature and number of pendant arms.[17]

Like L^5, L^6 has only one nitrile functionalised pendant arm but the macrocyclic framework is characterised by a bigger ring cavity with the introduction of an oxygen atom in the donor set. Binding of the NS$_2$-donors of the macrocyclic framework to Ag^I may seem most likely with this ligand due to the hard character of the O-donor. This would leave the O-centre non-co-ordinating thus favouring a four-coordinate quasi-tetrahedral structure around Ag^I by intervention of the nitrile group from a second molecule of L^6. A similar co-ordination behaviour towards Cu^I has been observed for some binucleating ligands based on [12]aneNS$_2$O.[18] In other words, there is no apparent obvious reason why L^6 should behave differently from L^5 in the interaction with Ag^I. Nevertheless, reaction of L^6 with Ag^I gives the discrete binuclear complex $[Ag_2(L^6)_2]^{2+}$ (Fig. 10).

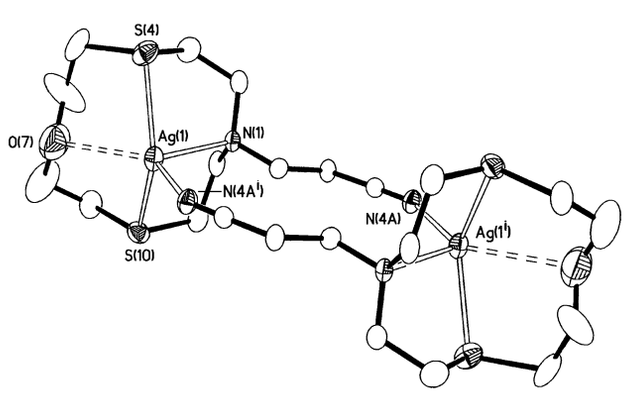

Fig. 10 View of the binuclear cation in $[Ag_2(L^6)_2][BF_4]_2$ with the numbering scheme adopted. Hydrogen atoms and counter ions are omitted for clarity and displacement ellipsoids are drawn at 30% probability [i = 2 − x, 2 − y, −z].

Each metal centre in the $[Ag_2(L^6)_2]^{2+}$ cation is co-ordinated by a [NS$_2$ + O] donor set from the [12]aneNS$_2$O macrocyclic framework of L^6 and by the nitrile group of a symmetry-related $[Ag(L^6)]^+$ unit. The Ag–N bond distance involving the bridging nitrile group is again the shortest in the co-ordination sphere of the Ag^I ion [Ag(1)–N($4A^i$) 2.266(4) Å, (Table 6)], but it is significantly longer than the corresponding bond lengths in $[Ag_2(L^4)_2][BF_4]_2$ [Ag(1)–N(44^i) 2.166(2) Å (Table 4)] and $\{[Ag(L^5)]BF_4\}_\infty$ [Ag(1)–N(74^i) 2.153(4)Å (Table 5)]. The other Ag–N and Ag–S bond distances in $[Ag_2(L^6)_2]^{2+}$ are comparable with those observed in the $[Ag(L^5)]^+$ [Tables 5 and 6]. As expected, the weakest interaction with the Ag^I ion is from the O-donor of the macrocyclic framework [Ag(1)–O(7) 2.788(6) Å], and is responsible for the very distorted co-ordination geometry around the metal centre. This interaction forces the Ag^I ion to adopt a constrained non-tetrahedral co-ordination sphere and, together with solid state packing effects, may well be responsible for the formation of the discrete binuclear complex $[Ag_2(L^6)_2]^{2+}$ instead of one-dimensional polymeric chains as observed in $\{[Ag(L^5)]BF_4\}_\infty$.

The ligands L^7 and L^8 have been considered as representative examples of nitrile-functionalised derivatives of mixed oxa/aza macrocycles. They are characterised by pendant arms of different lengths and, as for L^1–L^5, by an inherent stereochemical mismatch between the co-ordination preferences of the Ag^I ion (octahedral or tetrahedral) and the macrocyclic frameworks (potentially three coordinate for [9]aneN$_3$, [9]aneN$_2$S and [9]aneNS$_2$ and five-coordinate for [15]aneO$_2$N$_3$). Reaction of L^7 with one molar equivalent of $AgBF_4$ in MeCN at room temperature for 3 h gives a white microcrystalline solid after addition of Et$_2$O to the reaction mixture. Analytical and mass spectrometric data for the product are consistent with the stoichiometry $[Ag(L^7)]BF_4$. Single crystals were grown by diffusion of Et$_2$O into a solution of the white product in MeCN. The crystal structure confirms the formation of a one-dimensional sinusoidal polymer, $\{[Ag(L^7)]BF_4\}_\infty$, in which the repeat unit is the moiety $[Ag(L^7)]^+$ (Fig. 11, Table 7). Each Ag^I

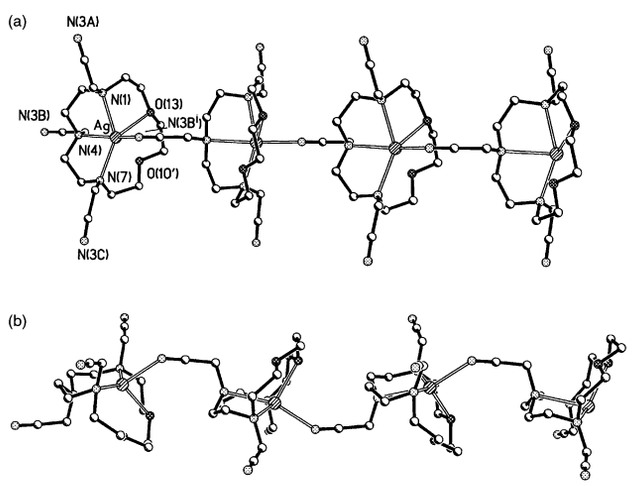

Fig. 11 a) Packing diagram for the $\{[Ag(L^7)]^+\}_\infty$ polymeric chain running along the [101] direction with the numbering scheme adopted. Hydrogen atoms and counter anions are omitted for clarity [i = −½ + x, $\frac{3}{2}$ − y, −½ + z]. Only one component of the disordered macrocyclic ligand is shown; b) complementary view of the $\{[Ag(L^7)]^+\}_\infty$ polymeric chain showing the sinusoidal pattern.

ion in the polymer shows a highly distorted octahedral co-ordination geometry with the equatorial positions occupied by two O- and two N-donors from the macrocyclic ring [Ag–O 2.514(4), 2.618(5) Å; Ag–N 2.398(4), 2.413(4) Å]. The axial positions are occupied by two N-donors, one from the

Table 7 Selected bond distances (Å) and angles (°) for $\{[Ag(L^7)]BF_4\}_\infty$

Ag–N(1)	2.413(4)	Ag–N(4)	2.559(4)
Ag–N(7)	2.398(4)	Ag–O(10′)	2.618(5)
Ag–O(13)	2.514(4)	Ag–N($3B^i$)	2.377(5)
N(1)–Ag–N(4)	75.37(13)	N(1)–Ag–N(7)	143.4(2)
N(1)–Ag–N($3B^i$)	96.4(2)	N(1)–Ag–O(13)	2.514(4)
N(1)–Ag–O(10′)	128.4(2)	N(4)–Ag–N(7)	75.17(14)
N(4)–Ag–N($3B^i$)	158.8(2)	N(4)–Ag–O(10′)	85.7(2)
N(4)–Ag–O(13)	104.16(13)	N(7)–Ag–N($3B^i$)	103.3(2)
N(7)–Ag–O(10′)	70.0(2)	N(7)–Ag–O(13)	135.46(14)
O(10′)–Ag–N($3B^i$)	114.0(2)	O(13)–Ag–N($3B^i$)	91.8(2)
O(10′)–Ag–O(13)	65.58(14)		

Symmetry operations: i = $-\frac{1}{2} + x, \frac{3}{2} - y, -\frac{1}{2} + z$.

Table 8 Selected bond distances (Å) and angles (°) for $[Ag(L^8)]PF_2O_2$

Ag–N(1)	2.445(2)	Ag–N(7)	2.464(2)
Ag–O(1)	2.458(2)	Ag–O(10)	2.656(2)
Ag–O(13)	2.612(2)		
N(1)–Ag–N(4)	74.94(6)	N(1)–Ag–N(7)	147.04(6)
N(1)–Ag–O(1)	109.43(6)	N(1)–Ag–O(10)	135.73(6)
N(1)–Ag–O(13)	70.84(5)	N(4)–Ag–N(7)	74.87(6)
N(4)–Ag–O(1)	146.79(6)	N(4)–Ag–O(10)	116.82(5)
N(4)–Ag–O(13)	106.99(5)	N(7)–Ag–O(1)	89.25(6)
N(7)–Ag–O(10)	71.26(6)	N(7)–Ag–O(13)	131.41(6)
O(1)–Ag–O(10)	83.78(6)	O(1)–Ag–O(13)	105.38(6)
O(10)–Ag–O(13)	64.90(5)		

$[15]aneO_2N_3$ framework [Ag–N(4) 2.559(4) Å] and the other from the nitrile group of one of the three pendant arms of a symmetry-related $[Ag(L^7)]^+$ unit [Ag–N($3B^i$) 2.377(5) Å, N(4)–Ag–N($3B^i$) 158.8(2)°]. The other two pendant arms of each $[Ag(L^7)]^+$ moiety are unbound and are directed away from the polymeric chain which runs along the [101] direction. The polymeric structure of $\{[Ag(L^7)]^+\}_\infty$ resembles that of $\{[Ag(L^5)]\}_\infty$ (Fig. 9), the major difference being the co-ordination environment around the metal centre, octahedral in $\{[Ag(L^7)]^+\}_\infty$ and tetrahedral in $\{[Ag(L^5)]\}_\infty$.

In order to ascertain whether pendant arms of a different length could also have dramatic effects on the co-ordination chemistry of nitrile-functionalised derivatives of $[15]aneO_2N_3$, we treated L^8 with $AgBF_4$ under the same experimental conditions as used for L^7. Unfortunately, only oils were recovered from this reaction. On changing the counter anion, however, by reacting L^8 with one molar equivalent of $AgPF_6$ in MeCN at room temperature colourless columnar crystals could be obtained upon diffusion of Et_2O vapour into the reaction mixture. An X-ray diffraction analysis confirms the formation of a discrete neutral mononuclear product with the formulation $[Ag(L^8)]PO_2F_2$. As in $\{[Ag(L^7)]BF_4\}_\infty$, the Ag^I ion in $[Ag(L^8)]$-PO_2F_2 shows a very distorted octahedral co-ordination sphere (Fig. 12, Table 8) with one of the axial positions being occupied by an O-atom of the $PF_2O_2^-$ formed by *in situ* hydrolysis of PF_6^-. This may explain the failure to obtain a crystalline product from the reaction of L^8 with $AgBF_4$.

Conclusions

Nitrile-functionalised derivatives of the macrocyclic ligands $[9]aneN_3$, $[9]aneN_2S$, $[9]aneNS_2$, $[12]aneNS_2O$ and $[15]aneO_2N_3$ show great promise as ligands for the synthesis of extended multidimensional inorganic polymers with metal ions such as Ag^I. Generally, the nitrile groups play an active role by linking different metal centres. The dimensionality of the resultant inorganic polymers is strictly dependent upon the number of the nitrile functionalised pendant arms present in the ligand, upon their length and upon the donor set and ring cavity of the macrocyclic framework. The results reported herein confirm the efficacy of new multidentate macrocyclic ligands designed for use as building blocks in crystal engineering.

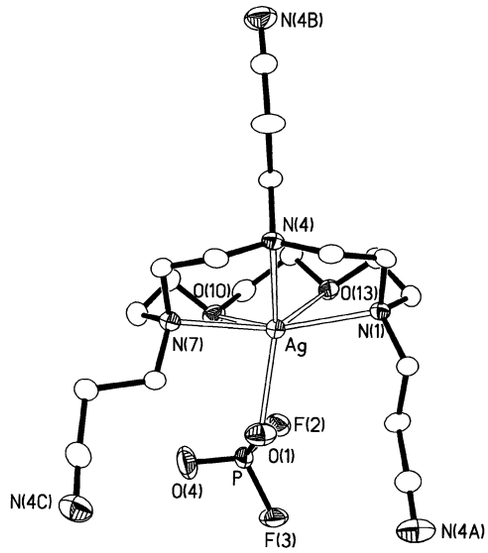

Fig. 12 View of $[Ag(L^8)]PF_2O_2$ with the numbering scheme adopted. Hydrogen atoms are omitted for clarity and displacement ellipsoids are drawn at 50% probability.

Experimental

1,4,7-Triazacyclononane ($[9]aneN_3$),[19] 1,2-bis[4,7-bis(2-cyanoethyl)-1,4,7-triazacyclonon-1yl]ethane (L^3),[20] 1-thia-4,7-diazacyclononane ($[9]aneN_2S$),[21] 1,4-dithia-7-azacyclononane ($[9]aneNS_2$),[22] 1,4,7-triaza-10,13-dioxacyclopentadecane ($[15]aneN_2O_3$,[23] and 1,4,7-tris (cyanomethyl)-1,4,7-triaza-10,13-dioxacyclopentadecane (L^7)[24] were prepared according to procedures reported in the literature. 4,7-Bis(2-cyanoethyl)-1-thia-4,7-diazacyclononane (L^4) was also prepared according to literature procedures,[25] but we have been able to isolate, purify and fully characterise this ligand for the first time. All starting materials were obtained from Aldrich and were used without further purification. Microanalyses were performed by the University of Nottingham School of Chemistry Microanalytical Service. IR spectra were recorded as KBr discs using a Perkin-Elmer 598 spectrometer over the range 200–4000 cm^{-1}. Fast atom bombardment (FAB), electron impact (EI) and electrospry (ES) mass spectra were recorded at the EPSRC Centre for Mass Spectroscopy at the University of Swansea.

Syntheses

1,4,7-Tris(cyanomethyl)-1,4,7-triazacyclononane (L^1). A mixture of $[9]aneN_3 \cdot 3HBr$ (3.0 g, 8.07 mmol), chloroacetonitrile (1.9 g, 25.2 mmol) and Et_3N (10 g, 0.099 mol) in EtOH (150 cm^3) was refluxed under N_2 for 24 h. After cooling, the solvent was removed under reduced pressure to yield a red oil which was dissolved in $CHCl_3$ (100 cm^3) and washed with H_2O (3 × 100 cm^3). The organic phases were collected and dried over $MgSO_4$. After filtration, the solvent was removed under reduced pressure to give a pale yellow solid (1.05 g, 53% yield). Elemental analysis, ^1H NMR and ^{13}C NMR spectra of this compound are reported in ref. 14. Mp: 94–96 °C. EI^+ mass spectrum *m/z*: 163 [$M^+ - 2(CH_2CN)$], 138 [$M^+ - 2(CH_2CN) - CN$] and 124 [$M^+ - 3(CH_2CN)$]. IR spectrum (KBr disk): *ν* 2937m, 2840m, 2227m, 1455m, 1132w, 1099w, 887w, 844w cm^{-1}.

1,4,7-Tris(2-cyanoethyl)-1,4,7-triazacyclononane (L^2). A mixture of $[9]aneN_3$ (0.52 g, 4.06 mmol) and acrylonitrile (30 cm^3) was refluxed overnight under a N_2 atmosphere. The solvent was removed under reduced pressure and the resulting

yellow oil was purified by flash chromatography on silica gel using THF as eluant. On removal of the solvent from the collected fractions a pale yellow solid was obtained (1.19 g, 95% yield). CHN, ^{1}H NMR and ^{13}C NMR spectra of this compound are reported in ref. 14. Mp: 50–52 °C. EI$^+$ mass spectrum *m*/*z*: 248 [$M^+ - CH_2CN$), 234 [$M^+ - C_2H_4CN$]. IR spectrum (KBr disk): *v* 2922m, 2811m, 2244s, 1455m, 1422w, 1361s, 1305w, 1133m, 1105s, 1022m, 994w, 872w, 744w cm^{-1}.

4,7-Bis(2-cyanoethyl)-1-thia-4,7-diazacyclononane (L^4). A mixture of [9]aneN_2S (0.843 g, 5.78 mmol) and acrylonitrile (30 cm^3) was stirred at 77 °C overnight. After cooling the solvent was removed *in vacuo* leaving a yellow–orange oil. The oil was passed through a silica gel column using THF as eluant. On removing the solvent a pale yellow solid was obtained (1.21 g, 83% yield). Mp: 80–82 °C. Found (calc. for $C_{12}H_{20}N_4S$): C, 57.42 (57.11); H, 8.26 (7.99); N, 21.93 (22.20%). EI$^+$ mass spectrum *m*/*z*: 253 [MH^+], 227 [$MH^+ - CN$]. ^{1}H NMR ($CDCl_3$, 300.1 MHz): δ_H 2.50 (4H, t, *J* = 6.67 Hz, NCH_2CH_2CN), 2.71 (4H, s, NCH_2CH_2N), 2.92 (4H, t, *J* = 6.71 Hz, NCH_2CH_2CN), 2.95–3.05 (8H, m, NCH_2CH_2S and NCH_2CH_2S). ^{13}C NMR ($CDCl_3$, 75.47 MHz): δ_C 16.91 (CH_2CN), 31.38 (NCH_2CH_2S), 53.93 (NCH_2CH_2S), 56.27, 59.14 (NCH_2CH_2N and NCH_2CH_2CN), 119.18 (*C*N). IR spectrum (KBr disk): *v* 2908s, 2848m, 2802s, 2241s, 1460m, 1436s, 1367s, 1332s, 1317s, 1278m, 1260m, 1218w, 1159w, 1136s, 1120s, 1044s, 1010m, 969m, 920m, 829w, 753w, 684w, 581m, 503m cm^{-1}.

7-(2-Cyanoethyl)-7-aza-1,4-dithiacyclononane (L^5). A mixture of [9]aneNS_2 (1.00 g, 6.12 mmol) and acrylonitrile (30 cm^3) was stirred at 77 °C overnight. The solvent was removed *in vacuo* to give a yellow–orange oil, which was purified by flash chromatography on silica gel using CH_2Cl_2 as eluant. On removal of the solvent from the collected fractions a colourless oil was obtained (1.04 g, 78% yield). Elemental analysis, ^{1}H NMR, ^{13}C NMR and IR spectra of this compound are reported in ref. 17. EI$^+$ mass spectrum *m*/*z*: 216 [M^+].

1-(2-Cyanoethyl)-1-aza-4,10-dithia-7-oxacyclododecane (L^6). A mixture of [12]aneNS_2O prepared according to the procedure described in ref. 26 (0.5 g, 2.4 mmol) and acrylonitrile (12 cm^3) was stirred at 77 °C for 24 h. The solvent was removed *in vacuo* to give a pale yellow solid (0.59 g, 96% yield). Mp: 66 °C. Found (calc. for $C_{11}H_{20}N_2OS_2$): C, 50.93 (50.73); H, 8.36 (7.74); N, 10.68 (10.76%). EI$^+$ mass spectrum: *m*/*z*: 260 [M^+], 220 [$M^+ - CH_2CN$]. ^{1}H NMR ($CDCl_3$, 300.1 MHz): δ_H 2.41 (2H CH_2CN, t, *J* = 6.97 Hz), 2.68 (4H, NCH_2CH_2S, t, *J* = 4.70 Hz), 2.80 (10H, m, CH_2SCH_2 and NCH_2CH_2CN), 3.71 (4H, CH_2OCH_2, t, *J* = 4.65 Hz). ^{13}C NMR ($CDCl_3$, 75.47 MHz): δ_C 16.97 (CH_2CN), 28.80 and 30.56 (CH_2SCH_2), 50.90 (NCH_2CH_2CN), 51.53 (CH_2NCH_2), 74.27 (CH_2OCH_2), 118.65 (*C*N). IR spectrum (KBr disk): *v* 2930s, 2860s, 2250m, 1460m, 1410m, 1295m, 1260m, 1135s, 1110s, 790m, 750m, 655m, cm^{-1}.

1,4,7-Tris(cyanoethyl)-1,4,7-triaza-10,13-dioxacyclopentadecane (L^8). [15]aneN_3O_2 (0.22 g, 1.01 mmol) was refluxed in acrylonitrile (20 cm^3) under N_2 for 16 h. After cooling, the solvent was removed by rotary evaporation to yield a colourless oil which was dried *in vacuo* (0.29 g, 77% yield). Found (calc. for $C_{19}H_{32}N_6O_2$): C, 60.40 (60.61); H, 8.40 (8.57); N, 22.20 (22.32%). EI$^+$ mass spectrum: *m*/*z*: 376 [M^+], 350 [$M^+ - CN$], 321 [$M^+ - CH_2CH_2CN$]. ^{1}H NMR ($CDCl_3$, 300.1 MHz): δ_H 3.59 (4H, s, OCH_2) 3.58 (4H, t, *J* = 4.70 Hz, OCH_2CH_2N), 2.80 (4H, t, *J* = 4.70 Hz, OCH_2CH_2N), 2.75 (8H, t, *J* = 5.16 Hz, NCH_2), 2.88 (6H, t, *J* = 6.77 Hz, CH_2CH_2CN), 2.45 (6H, t, *J* = 6.77 Hz, CH_2CH_2CN). ^{13}C NMR ($CDCl_3$, 75.47 MHz): δ_C 17.1 (CH_2CN), 16.9 (CH_2CN), 51.4 (NCH_2CH_2CN), 51.5 (NCH_2CH_2CN), 52.9 (NCH_2CH_2N), 53.1 (NCH_2CH_2N), 54.0 (OCH_2CH_2N), 70.6 (OCH_2CH_2N), 70.8 (OCH_2), 119.1 (*C*N). IR spectrum (KBr disk): *v* 2924m, 2853m, 2246m, 1459m, 1384m, 1113s, 801m cm^{-1}.

{[Ag(L^1)][PF_6]}$_\infty$. A mixture of $AgPF_6$ (19.5 mg, 0.077 mmol) and 1,4,7-tris(cyanomethyl)-1,4,7-triazacyclononane (L^1) (19.0 mg, 0.077 mmol) in MeCN (15cm^3) was stirred for 3 h at room temperature. The solvent was partially removed under reduced pressure and Et_2O vapour was allowed to diffuse into the remaining solution. Colourless crystals suitable for X-ray structural analysis were obtained (28.9 mg, 75.3% yield). Mp: 212–214 °C. Found (calc. for $C_{12}H_{18}AgF_6N_6P$): C, 29.10 (28.88); H, 3.83 (3.63); N, 19.15 (18.84%). FAB mass spectrum (3-nitrobenzyl alcohol [3-NOBA] matrix) *m*/*z*: 353 for [^{107}Ag(L^1)]$^+$. ^{1}H NMR (CD_3CN, 300.1 MHz, 298K): δ_H 2.14 (12H, s, NCH_2CH_2N), 2.75 (6H, s, NCH_2CN). IR spectrum (KBr disc): *v* 2930 m, 2843 s, 2247 (s, CN stretch), 1457 s, 1337 s, 1113 s, 995 s, 881 s.

{[Ag(L^1)][BF_4]}$_\infty$. $AgBF_4$ (15.0 mg, 0.077 mmol) was dissolved in MeCN (15 cm^3) and a solution of 1,4,7-tris(cyanomethyl)-1,4,7-triazacyclononane (L^1) (19.0 mg, 0.077 mmol) in MeCN (15 cm^3) was added dropwise. The solution was stirred for 3 h at room temperature. Single crystals suitable for X-ray structural analysis were obtained by diffusion of Et_2O vapour into a solution of the complex in MeCN at room temperature (24.2 mg, 71.4% yield). Found (calc. for $C_{12}H_{18}AgBF_4N_6$): C, 32.8 (32.68); H, 4.0 (4.11); N, 19.1 (19.06%). FAB mass spectrum (3-NOBA matrix) *m*/*z* : 353 for [^{107}Ag(L^1)]$^+$. IR spectrum (KBr disc): *v* 2925 m, 2873 m, 2245 (m, CN stretch), 1384 s, 1084 s.

{[Ag_2(L^2)$_2$][BF_4]$_2$}$_\infty$. A mixture of 1,4,7-tris(cyanoethyl)-1,4,7-triazacyclononane (L^2) (25 mg, 0.087 mmol) and $AgBF_4$ (16.94 mg, 0.087 mmol) in MeCN (5 cm^3) was stirred in the dark at room temperature for 2 h. The solvent was partially removed under reduced pressure and the product crystallised by diffusion of Et_2O vapour into the reaction solution (27 mg, 64.4% yield). Mp 160–162 °C. Found (calc. for $C_{15}H_{24}AgBF_4N_6$): C, 36.85 (37.29); H, 4.85 (5.00); N, 17.77 (17.40%). FAB mass spectrum (3-NOBA matrix): *m*/*z* 395; calc. for [^{107}Ag(L^2)]$^+$ 395. ^{1}H NMR (CD_3CN, 300.1 MHz, 298 K): δ_H 2.67 (12H, s, NCH_2CH_2N), 2.71 (6H, t, *J* = 7.37 Hz, NCH_2CH_2CN), 3.01 (6H, t, *J* = 7.31 Hz, NCH_2CH_2CN). IR spectrum (KBr disc): *v* 2952m, 2902m, 2835m, 2247m, 1496w, 1464m, 1417m, 1374m, 1285m, 1253w, 1054s, 999m, 942w, 895w cm^{-1}.

{[Ag_2(L^3)][PF_6]$_2$}$_\infty$. A mixture of 1,2-bis[4,7-bis(2-cyanoethyl)1,4,7-triazacyclonon-1-yl]ethane (L^3) (16.5 mg, 0.0332 mmol) and $AgPF_6$ (16.8 mg, 0.0664 mmol) in MeCN (7 cm^3) was stirred at room temperature in the dark for 4 h. Crystals suitable for diffraction studies were obtained by diffusing Et_2O vapour into a solution of the complex in MeCN. Found (calc. for $C_{13}H_{22}AgN_5PF_6$): C, 30.95 (31.15); H, 4.20 (4.42); N, 1.88 (13.97%). FAB mass spectrum (3-NOBA matrix): *m*/*z* 857, 711, 603; calc. for [$^{107}Ag_2(L^3)PF_6]^+$, [$^{107}Ag_2(L^3)]^+$ and [^{107}Ag(L^3)]$^+$ 855, 710 and 603 respectively. ^{1}H NMR (CD_3CN, 300.1 MHz, 298 K): δ_H 3.05 (8H, t, *J* = 7.1 Hz, NCH_2CH_2CN), 2.94–2.92 (24H, m, ring CH_2), 2.83 (4H, s, CH_2 bridging [9]aneN_3 moieties), 2.65 (8H, t, *J* = 7.1 Hz, NCH_2CH_2CN). IR spectrum (KBr disc): *v* 2950m, 2922m, 2844m, 2249m, 1057m, 1494s, 1466m, 1315s, 1153m, 1135s, 842s, 755s, 689w, 557w, 482m cm^{-1}.

[Ag_2(L^4)$_2$][BF_4]$_2$. A mixture of 4,7-bis(2-cyanoethyl)-1-thia-4,7-diazacyclononane (L^4) (30 mg, 0.119 mmol) and $AgBF_4$ (23.16 mg, 0.119 mmol) in MeCN (5 cm^3) was stirred at room temperature for 12 h. The solvent was partially removed under reduced pressure and Et_2O vapour was allowed to diffuse into the remaining solution. Colourless block crystals of the title complex were obtained (50.4 mg, 95% yield). Mp: at 141 °C the

compound turns black, melting fully at 162 °C. Found (calc. for $C_{12}H_{20}AgBF_4N_4S$): C, 31.98 (32.30); H, 4.20 (4.52); N, 12.10 (12.56%). FAB mass spectrum (3-NOBA matrix): *m*/*z* 807, 359; calc. for $[^{107}Ag_2(L^4)_2(BF_4)]^+$ and $[^{107}Ag(L^4)]^+$ 805 and 359 respectively. ^{1}H NMR (CD_3CN, 300.1 MHz, 298 K): δ_H 2.66 (4H, s, NCH_2CH_2N), 2.67–2.73 (8H, m), 2.84 (4H, t, J = 5.81 Hz), 3.07 (4H, t, J = 7.28 Hz). IR spectrum (KBr disc): *ν* 2922m, 2822m, 2267m, 2233w, 1478m, 1456m, 1417m, 1367m, 1305w, 1283m, 1055s, 972m, 850w, 761w, 733w, 600w, 517w cm^{-1}.

{[Ag(L^5)]BF$_4$}$_\infty$. A mixture of 7-(2-cyanoethyl)-7-aza-1,4-dithiacyclononane (L^5) (20 mg, 0.1085 mmol) and $AgBF_4$ (21.13 mg, 0.1085 mmol) in MeCN (5 cm^3) was stirred at room temperature in the dark for 4 h. Crystals of good quality were obtained by slow evaporation (21 mg, 47% yield). Mp: 204 °C with decomposition. Found (calc. for $C_9H_{16}AgBF_4N_2S_2$): C, 25.95 (26.27); H, 3.54 (3.90); N, 6.65 (6.81%). FAB mass spectrum (3-NOBA matrix): *m*/*z* 323; calc. for $[^{107}Ag(L^5)]^+$ 323. ^{1}H NMR (CD_3CN, 300.1 MHz, 298 K): δ_H 2.60–2.72 (6H, m), 2.74–2.83 (4H, m), 2.87 (4H, s, SCH_2CH_2S), 3.10 (2H, t, J = 7.43 Hz). IR spectrum (KBr disc): *ν* 2920m, 2849m, 2794m, 2290m, 2244m, 1467m, 1411m, 1360m, 1333w, 1300m, 1055s, 900m, 833w, 812w, 745w, 664w, 618w, 580w, 521m cm^{-1}.

[Ag$_2$(L^6)$_2$][BF$_4$]$_2$. A mixture of 1-(2-cyanoethyl)-1-aza-4,10-dithia-7-oxacyclododecane (L^6) (30 mg, 0.115 mmol) and $AgBF_4$ (22.5 mg, 0.115 mmol) in MeCN (5 cm^3) was stirred at room temperature for 4 h. The solvent was partially removed under reduced pressure and Et_2O vapour was allowed to diffuse into the remaining solution. Colourless prismatic crystals of the title complex were obtained (35 mg, 66.6% yield). Mp: 212–215 °C with decomposition. Found (calc. for $C_{11}H_{20}AgBF_4N_2OS_2$): C, 28.95 (29.03); H, 4.37 (4.43); N, 6.10 (6.16%). IR spectrum (KBr disc): *ν* 2910m, 2820m, 2270m, 1420m, 1300m, 1090m cm^{-1}.

[Ag(L^7)]BF$_4$. $AgBF_4$ (16.0 mg, 0.082 mmol) was dissolved in MeCN (15 cm^3) and a solution of L^7 (27.4 mg, 0.082 mmol) in MeCN (15 cm^3) was added dropwise. The solution was stirred for 3 h at room temperature. Addition of Et_2O yielded a white solid (34.3 mg, 79.3% yield). Single crystals suitable for X-ray structural analysis were obtained by diffusion of Et_2O vapour into a solution of the complex in MeCN at room temperature. Found (calc. for $C_{16}H_{26}Ag\,BF_4N_6O_2$): C, 36.40(36.32); H, 5.0(4.95); N, 14.5(14.36%). FAB mass spectrum (3-NOBA matrix) *m*/*z*: 441; calc. for $[^{107}Ag(L^7)BF_4]^+$ 441. ^{1}H NMR (CD_3CN, 300.1 MHz, 298 K): δ_H 3.64 (4H, s, OCH_2), 3.59 (4H, t, J = 4.63 Hz, OCH_2CH_2N), 2.88 (4H, t, J = 4.63 Hz, OCH_2CH_2N), 2.79 (8H, s, NCH_2), 3.81 (4H, s, NCH_2CN), 3.82 (2H, s, NCH_2CN). IR spectrum (KBr disc): *ν* 2920m, 2858m, 2238m, 1384s, 1084s cm^{-1}.

[Ag(L^8)]PF$_2$O$_2$. $AgPF_6$ (18.2 mg, 0.072 mmol) was dissolved in MeCN (15 cm^3) and a solution of 1,4,7-tris(cyanoethyl)-1,4,7-triaza-10,13-dioxacyclopentadecane (L^8) (27.1 mg, 0.072 mmol) in MeCN (15 cm^3) was added dropwise. The solution was stirred for 3 h at room temperature. Single crystals suitable for X-ray structural analysis were obtained by diffusion of Et_2O vapour into a solution of the complex in MeCN at room temperature (19.9 mg, 47.8% yield). Found (calc. for $C_{19}H_{32}AgF_2N_6O_4P$): C, 38.75 (38.99); H, 5.63 (5.51); N, 14.25 (14.36%). ES$^+$ mass spectrum *m*/*z*: 483; calc. for $[^{107}Ag(L^8)]^+$ 484 (the $PF_2O_2^-$ anion was also detected: *m*/*z*: 101). ^{1}H NMR (CD_3CN, 300.1 MHz, 298 K): δ_H 3.62 (4H, s, OCH_2), 3.56 (4H, t, J = 4.37 Hz, OCH_2CH_2N), 2.76 (4H, t, J = 4.37 Hz, OCH_2CH_2N), 2.68 (8H, s NCH_2), 3.11 (2H, t, J = 7.33 Hz, CH_2CH_2CN), 3.04 (4H, t, J = 7.22 Hz, CH_2CH_2CN), 2.63 (4H, t, J = 7.22 Hz, CH_2CH_2CN), 2.54 (2H, t, J = 7.33, CH_2CH_2CN). IR spectrum (KBr disc): *ν* 2854s, 2246m, 1312s, 1160s, 850s, 498s cm^{-1}.

Table 9 Summary of crystal data

Compound	{[Ag(L^1)]BF$_4$}$_\infty$	{[Ag$_2$(L^3)][PF$_6$]$_2$}$_\infty$	[Ag$_2$(L^4)$_2$][BF$_4$]$_2$	{[Ag(L^5)]BF$_4$}$_\infty$	[Ag$_2$(L^6)$_2$][BF$_4$]$_2$	{[Ag(L^7)]BF$_4$}$_\infty$	[Ag(L^8)]PO$_2$F$_2$
Formula	$C_{12}H_{18}AgBF_4N_6$	$C_{26}H_{44}Ag_2F_{12}N_{10}P_2$	$C_{12}H_{20}AgBF_4N_4S$	$C_9H_{16}AgBF_4N_2S_2$	$C_{11}H_{20}AgBF_4N_2OS_2$	$C_{16}H_{26}AgBF_4N_6O_2$	$C_9H_{32}AgF_2N_6O_4P$
M	441.00	1002.39	447.06	411.04	455.09	529.11	585.35
Crystal size/mm	0.45 × 0.24 × 0.22	0.60 × 0.54 × 0.15	0.50 × 0.20 × 0.19	0.64 × 0.60 × 0.13	0.20 × 0.15 × 0.08	0.30 × 0.12 × 0.06	0.32 × 0.15 × 0.08
Crystal system	Monoclinic	Triclinic	Monoclinic	Monoclinic	Monoclinic	Monoclinic	Monoclinic
Space group	$P2_1/n$ (no. 14)	$P\bar{1}$ (no. 2)	$P2_1/c$ (no. 14)	$C2/c$ (no. 15)	$P2_1/n$ (no. 14)	$P2_1/n$ (no. 14)	$P2_1/c$ (no. 14)
a/Å	10.314(1)	8.003(4)	7.6037(11)	31.961(5)	6.941(1)	9.876(1)	9.8248(4)
b/Å	14.846(2)	10.756(6)	13.542(2)	6.893(4)	21.102(2)	15.316(2)	14.6417(7)
c/Å	10.604(1)	11.083(7)	15.674(2)	13.144(2)	11.534(1)	14.823(2)	17.5430(8)
α/°		101.80(5)					
β/°	93.543(2)	101.96(5)	90.598(13)	92.00(1)	105.480(1)	108.022(2)	105.747(1)
γ/°		97.02(5)					
U/Å^3	1620.6(3)	900.0(9)	1613.8(4)	2894.0(18)	1628.1(3)	2132.1(5)	2428.9(2)
Z	4	1	4	8	4	4	4
D_{calc}/g cm^{-3}	1.807	1.849	1.856	1.887	1.857	1.648	1.601
T/K	150(2)	220(2)	150(2)	220(2)	293(2)	150(2)	150(2)
μ(Mo-Kα)/mm^{-1}	1.293	1.276	1.421	1.711	1.535	1.005	0.948
Reflections collected	14047	3463	2877	3165	4423	13541	15628
Unique reflections, R_{int}	3848, 0.020	3463, —	2848, 0.0488	2512, 0.0175	4423, —	5006, 0.0520	5930, 0.051
*R*1	0.0206	0.0385	0.0238	0.0405	0.0482	0.0476	0.0299
*w*R2 [all data]	0.0565	0.0993	0.0551	0.1162	0.1118	0.1360	0.0716
Parameters refined	217	235	208	212	219	263	298
$\Delta\rho_{max,\ min}$/e Å^{-3}	+0.71, −0.40	+0.92, −0.75	+0.45, −0.29	+0.80, −0.87	+1.19, −0.83	+1.02, −0.89	+0.81, −0.40

Crystallography

Crystal data and refinement details for $\{[Ag(L^1)]PF_6\}_\infty$ and $\{[Ag_2(L^2)_2][BF_4]_2\}_\infty$ are reported in ref. 14; those for all other structure determinations appear in Table 9. Only special features of the analysis are noted here. The crystals were cooled using an Oxford Cryosystem open-flow nitrogen cryostat.[27] Data were collected on a Stoë Stadi-4 four-circle diffractometer using ω–θ scans for $\{[Ag_2(L^3)][PF_6]_2\}_\infty$, $[Ag_2(L^4)_2][BF_4]_2$ and $\{[Ag(L^5)]BF_4\}_\infty$; for $\{[Ag(L^1)]BF_4\}_\infty$, $[Ag_2(L^6)_2][BF_4]_2$, $\{[Ag(L^7)]BF_4\}_\infty$ and $[Ag(L^8)]PF_2O_2$ data were collected on a Bruker SMART1000 CCD area detector diffractometer using ω scans. Data were corrected for Lorentz and polarisation effects and absorption corrections were applied using numerical or ψ-scan methods for the data collected on the Stoë Stadi-4 four circle diffractometer and semi-empirical methods[28] for the data collected on the Bruker SMART CCD area detector diffractometer. All the structures except $[Ag_2(L^6)_2][BF_4]_2$ were solved by direct methods using the SHELXS program[29] followed by difference Fourier synthesis. The structure of $[Ag_2(L^6)_2][BF_4]_2$ was solved by direct methods using the program SIR 97.[30] Except as noted below, all non-H atoms were refined anisotropically[31] and H atoms were introduced at calculated positions and thereafter incorporated into a riding model with $U_{iso}(H) = 1.2U_{eq}(C)$. The structures were developed by alternating cycles of least-squares refinement on F^2 and ΔF synthesis.[31] In $\{[Ag(L^7)]BF_4\}_\infty$ the BF_4^- ion and part of the [15]aneO_2N_3 framework were both found to be disordered. The disorder in the BF_4^- ion was modelled by two equally occupied sites for each F atom to give two tetrahedra coincident at the boron. The components were refined isotropically with restraints to impose tetrahedral geometry on each. The disorder in the macrocyclic ligand was modelled with C(5), C(6), C(8) and O(10) being modelled over two sites with the occupancy factor 0.65 for the major components of C(5), C(6) and C(8) and 0.7 for that of O(10). Appropriate restraints were applied to the bond lengths of the disordered portion of the macrocyclic ligand with both components being refined isotropically. In $[Ag_2(L^6)_2][BF_4]_2$, atoms C(6), O(7) and C(8) display quite high displacement parameters which may be indicative of partial disorder due to the presence of similar but different conformations. Any attempt to split each of these atoms into two components offered no advantage. However, appropriate restraints were applied to the C–C and C–O bond lengths in this region of the macrocyclic framework.

CCDC reference numbers 173745–173751.

See http://www.rsc.org/suppdata/dt/b1/b110134j/ for crystallographic data in CIF or other electronic format.

Acknowledgements

We thank the Engineering and Physical Sciences Research Council (UK) and the Ministero dell'Università e della Ricerca Scientifica e Tecnologica (M.U.R.S.T.), and the University of Nottingham for support. We thank the EPSRC National Service Centre for Mass Spectrometry at the University of Swansea for mass spectra.

References

1 S. R. Batten and R. Robson, *Angew. Chem., Int. Ed.*, 1998, **37**, 1460; P. J. Hagrman, D. Hagrman and J. Zubieta, *Angew. Chem., Int Ed.*, 1999, **38**, 2638; M. Eddaoudi, D. B. Moler, H. Li, B. Chen, T. M. Reineke, M. O'Keeffe and O. M. Yaghi, *Acc. Chem. Res.*, 2001, **34**, 319.
2 A. J. Blake, N. R. Champness, P. Hubberstey, W.-S. Li, M. Schröder and M. A. Withersby, *Coord. Chem. Rev.*, 1999, **183**, 117.
3 M. Fujita and K. Ogura, *Bull. Chem. Soc. Jpn.*, 1996, **69**, 1471.
4 L. Carlucci, G. Ciani, P. Macchi, D. M. Proserpio and S. Rizzato, *Chem. Eur. J.*, 1999, **5**, 237.
5 O. M. Yaghi, H. Li, C. Davis, D. Richardson and T. L. Groy, *Acc. Chem. Res.*, 1998, **31**, 474; M. Munakata, L. P. Wu and T. Kuroda-Sowa, *Adv. Inorg. Chem.*, 1998, **46**, 173.
6 M. A. Withersby, A. J. Blake, N. R. Champness, P. A. Cooke, P. Hubberstey and M. Schröder, *New. J. Chem.*, 1999, **23**, 573 and refs. therein.
7 A. N. Khlobystov, A. J. Blake, N. R. Champness, D. A. Lemenovskii, A. G. Majouga, N. V. Zyk and M. Schröder, *Coord. Chem. Rev.*, 2001, **222**, 137.
8 M. L. Tong, H. K. Lee, X.-M. Chen, R.-B. Huang and T. C. W. Mak, *J. Chem. Soc., Dalton Trans.*, 1999, 3657.
9 P. V. Bernhardt and G. A. Lawrence, *Coord. Chem. Rev.*, 1990, **104**, 297.
10 P. Chaughuri and K. Wieghardt, *Prog. Inorg. Chem.*, 1987, **35**, 329.
11 K. P. Wainwright, *Coord. Chem. Rev.*, 1997, **166**, 35.
12 F. H. Fry, B. Graham, L. Spiccia, D. C. R. Hockless and E. R. T. Tiekink, *J. Chem. Soc., Dalton Trans.*, 1997, 827 and refs. therein.
13 S. J. Brudenell, L. Spiccia, A. M. Bond, P. Comba and D. C. R. Hockeless, *Inorg. Chem.*, 1998, **37**, 3705.
14 L. Tei, V. Lippolis, A. J. Blake, P. A. Cooke and M. Schröder, *Chem. Commun.*, 1998, 2633; see also P. D. Beer and D. Gao, *Chem. Commun.*, 2000, 443; K. S. Min and M. P. Suh, *Chem. Eur. J.*, 2001, **7**, 303 and references therein.
15 L. Carlucci, G. Ciani, D. M. Proserpio and A. Sironi, *Angew. Chem., Int. Ed. Engl.*, 1995, **34**, 1895.
16 S. J. Brudenell, L. Spiccia and E. R. T. Tiekink, *Inorg. Chem.*, 1996, **35**, 1974; A. J. Blake, T. M. Donlevy, P. A. England, I. A. Fallis, S. Parsons, S. A. Ross and M. Schröder, *J. Chem. Soc., Chem. Commmun.*, 1994, 1981.
17 V. Lippolis, A. J. Blake, P. A. Cooke, F. Isaia, W.-S. Li and M. Schröder, *Chem. Eur. J.*, 1999, **5**, 1987.
18 M.-T. Youinou, J. A. Osborn, J.-P. Collin and P. Lagrange, *Inorg. Chem.*, 1986, **25**, 453.
19 J. E. Richman and T. J. Atkins, *J. Am. Chem. Soc.*, 1974, **96**, 2268.
20 A. J. Blake, J. P. Danks, W.-S. Li, V. Lippolis and M. Schröder, *J. Chem. Soc., Dalton Trans.*, 2000, 3035.
21 A. J. Blake, J. P. Danks, A. Harrison, S. Parsons, P. Schooler, G. Whittaker and M. Schröder, *J. Chem. Soc., Dalton Trans.*, 1998, 2335.
22 A. J. Blake, J. P. Danks, I. A. Fallis, A. Harrison, W.-S. Li, S. Parsons, S. A. Ross, G. Whittaker and M. Schröder, *J. Chem. Soc., Dalton Trans.*, 1998, 3969.
23 R. D. Hancock, R. Bhavan, P. W. Wade, J. C. A. Boeyens and S. M. Dobson, *Inorg. Chem.*, 1989, **28**, 187.
24 L. Tei, A. Bencini, A. J. Blake, B. Valtancoli, C. Wilson and M. Schröder, *J. Chem. Soc., Dalton Trans.*, 2000, 4122.
25 D. G. Fortier and A. McAuley, *Inorg. Chem.*, 1989, **28**, 655.
26 L. G. A. van de Water, F. ten Hoonte, W. L. Driessen, J. Reedijk and D. C. Sherrington, *Inorg. Chim. Acta*, 2000, **303**, 77.
27 J. Cosier and A. M. Glazer, *J. Appl. Crystallogr.*, 1986, **19**, 105.
28 SADABS Area-Detector Absorption Correction Program, Bruker AXS, Inc., Madison, WI, USA, 2000.
29 G. M. Sheldrick, SHELXS-86–97, Acta Crystallogr., Sect. A, 1990, **46**, 467.
30 A. Altomare, G. Cascarano, C. Giacovazzo, A. Guagliardi, M. C. Burla, G. Polidori and M. Camalli, *J. Appl. Crystallogr.*, 1994, **24**, 435.
31 G. M. Sheldrick, SHELXL-93–97, Universität Göttingen, Germany, 1997.